Generation of quasi-monoenergetic ion beams using short and intense laser pulses

Emmanuel d'Humières[1,2,3], Julien Fuchs[2], Toma Toncian[4], Patrizio Antici[2], Patrick Audebert[2], Marco Borghesi[5], Erik Brambrink[2], Carlo Alberto Cecchetti[4], Erik Lefebvre[6], Patrick Mora[3], Ariane Pipahl[4], Lorenzo Romagnani[2], Yasuhiko Sentoku[1], and Oswald Willi[4]

[1]*Nevada Terawatt Facility, Physics Department, MS-220, University of Nevada, Reno, Nevada 89557, USA*

[2]*Laboratoire pour l'Utilisation des Lasers Intenses, UMR 7605 CNRS-CEA-Ecole Polytechnique-Université Paris VI, 91128 Palaiseau, France*

[3]*Centre de Physique Théorique, UMR 7644 CNRS-Ecole Polytechnique, 91128 Palaiseau, France*

[4]*Heinrich Heine Universität Düsseldorf, D-40225 Düsseldorf, Germany*

[5]*School of Mathematics and Physics, The Queen's University Belfast, Belfast BT7 1NN, Northern Ireland, United Kingdom*

[6]*DPTA, CEA-DIF, Bruyères-le-Châtel, France*

Laser-accelerated ion sources have exceptional properties and could stimulate development of compact ion accelerators. For many applications beam control is an essential requirement. A new and interesting technique to control proton beam characteristics has been recently developed. It consists in using an ultrafast laser-triggered micro-lens, which provides simultaneous energy selection and focusing of the incoming ion beam and is tunable. Particle-in-cell simulations coupled with particle tracing are used to model the focusing and energy selection mechanisms, and to study the symmetry of the expanding plasma inside the micro-lens. The model developed is able to reproduce and explain the experimental results obtained at the Laboratoire pour l'Utilisation des Lasers Intenses in France.

OCIS codes: 350.4990, 350.5400.

In the last few years, intense research has been conducted on laser-accelerated ion sources and their applications. These sources have exceptional properties, i.e. high brightness, high spectral cut-off, high directionality and laminarity. These proton sources open new opportunities for ion beam generation and control, and could stimulate development for compact ion accelerators. For many applications beam control is an essential requirement. Focusing at short distances (hundreds of microns) has been achieved by curving the target surface in order to focus down the protons to a tight spot[1−3]. For energy selection, there are already several options. First, it has been proposed to use combinations of conventional deflecting magnets with selecting apertures to pick only a fraction of the broad initial energy distribution that is subsequently refocused for dose delivering[4]. Research at JAEA-KPSI (Japan) is exploring phase-space rotation. Alternatively, it is also possible to achieve energy selection by using double-layer targets with a heavy ion layer followed by a thin proton layer. This scheme has recently been demonstrated by using micro-structured targets[5,6]. A different and interesting option to solve the two issues mentioned above simultaneously is to use an ultrafast laser-triggered micro-lens[7]. This device provides tunable, simultaneous focusing and energy selection of MeV proton beams. The micro-lens is a hollow cylinder that is irradiated by an auxiliary laser pulse. This pulse injects relativistic electrons through the cylinder's wall. These electrons spread evenly on the cylinder's inner walls and initiate hot plasma expansion. The radially symmetric transient electric fields associated with the expansion can act to focus a fraction of the broadband proton beam (the fraction that transits at the time the device is switched) along the axis of the cylinder. This broadband beam is the one accelerated by a primary laser beam from the source foil. Its operation was demonstrated in experiments carried out at the Laboratoire pour l'Utilisation des Lasers Intenses (LULI), in France, employing the 100-TW laser providing two independently compressed chirped-pulse amplification (CPA) pulses. Particle-in-cell (PIC) simulations and new experiments are used here to explain the focusing and energy selection mechanisms, and to study the symmetry of the expanding plasma inside the cylinder.

We have performed PIC simulations and particle tracing of the collimated protons using the actual scale of the cylinder and the actual beam properties at the source, as reported in Ref. [7]. We observed a very good agreement between these simulations and the experimental results therein, thus supporting strongly our above interpretation of the features and capabilities of the micro-lens. The ion peak at 6 MeV (see Fig. 4 of Ref. [7]) and the density depression at the energies lower than the peak are both reproduced. The simulations investigate the plasma expansion from a 700-μm diameter cylinder and the propagation through the cylinder of protons emitted from the source, using the measured beam divergence and energy spectrum. This allows us to understand better the way the micro-lens works. First, the laser pulse triggering the micro-lens, focused on the cylinder's outer wall, generates a population of hot electrons that spread evenly on the cylinder's walls (as demonstrated by the two-dimentional (2D) PIC simulation detailed at the end of this letter). Then, these electrons form a Debye sheath at the inner wall, pull out ions and induce plasma flow into vacuum as we have shown in a recent paper where the ion front

was measured on laser irradiated planar targets[8]. We describe this expansion with a one-dimentional (1D) PIC simulation performed with the code CALDER[9,10] considering plasma evolution along a cylinder's diameter (i.e. transversely to the cylinder's axis). The cylinder is modelled as 2 slabs of plasma separated by the cylinder's diameter. A fast-evolving charge-separation electric field arises inside the cylinder, associated with the plasma flow from the micro-lens. This field is the cause of the observed focusing/collimation of the protons passing through the micro-lens. We then track the trajectories of the protons transiting through this field developed within the micro-lens.

The effect on the protons varies depending on parameters such as proton energy, proton transit time, and field strength, and therefore focusing effects are inherently transient. The snapshot of the protons trajectories propagating through the micro-lens in Fig. 1 corresponds to the experimental configuration used to measure the spectrum shown in Fig. 4 of Ref. [7]. In these simulations, we reproduce the plasma flow from a 700-μm-diameter cylinder and we propagate protons through the spatio-temporal dependent resulting fields. As in the experiment, the protons are produced at 4 mm from the front of the cylinder (at $x = -4000$ μm) and located at the middle of the left boundary of the simulation box ($y = 2547$ μm). They propagate through the cylinder that is placed between $x = 0$ and $x = 3000$ μm. The cylinder, which has a thickness of 50 μm, is irradiated by a laser pulse at an intensity 3×10^{18} W/cm^2, and with a pulse duration of 350 fs. The initial electron temperature considered in the PIC simulation is estimated from the pulse's ponderomotive potential, the initial electron density is estimated by considering that a known fraction (i.e. 40 %, inferred from experimental data) of the laser energy is converted in the hot electrons and then they spread evenly on the cylinder's walls. So the hot-electron density is approximately 6×10^{-5} n_c, where n_c is the critical density at λ=1 μm. We consider that when the plasma expansion starts, the field obtained in the PIC simulation is the same for all $x \in [0, 3000]$ (μm). Protons at 7.6 MeV enter the cylinder 96 ps before it is triggered (i.e. they exit the cylinder before it is triggered). These protons retain their initial large divergence. Protons at 6.25 MeV enter the cylinder 83 ps before it is triggered. These protons are clearly collimated (Fig. 2) and therefore induce a strong peak in the spectrum after having passed through the spectrometer slit. Protons at 4.9 MeV enter the cylinder 64 ps before it is triggered (i.e. they are closer to the middle of the cylinder when it is triggered), so they see a stronger field than the 6-MeV protons along their path in the cylinder. As a consequence, these protons are actually focused tightly at a very short distance from the micro-lens exit plane and diverge also strongly after this focusing point. This explains why there is a dip in the spectrum at this energy and below.

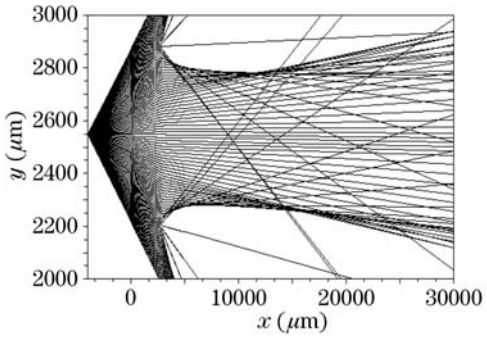

Fig. 1. Trajectories for 100 protons at 6.25 MeV. The protons enter the cylinder 83 ps before it is triggered. The two axes are not scaled similarly for clarity.

A 2D simulation using CALDER was performed, starting with a hot cylinder with the same parameters as above and the same plasma conditions. The evolution of the field in the 2D simulation is similar to the one in the 1D simulation, which is therefore sufficient to calculate the evolution of the electrostatic field inside the cylinder, which is then used for particle tracing. Indeed, the size of the cylinder reduces the difference between a cylindrical expansion and a planar expansion. The initial hypothesis of an even spread of the hot electrons around the cylinder is tested later in this letter.

We performed a proof-of-principle experiment of the performance of the micro-lens in collimating and energy selecting of proton beams, and modelled successfully its operation. Now, the device's performance can be reliably scaled to higher energies, as showed by simulations (Fig. 2). It can be achieved using laser pulses with currently available specifications to trigger the ion lens. A secondary laser with an intensity of 10^{20} W/cm^2, and a pulse duration of 700 fs, can efficiently focus 270-MeV protons. We have observed that there is a dependence of the "focal length" of the micro-lens as a function of the input proton energy and transit time through the micro-lens. This shows that this device has also potential for conventional ion beams handling apart from the prospects offered by hadrontherapy. However, the generation of laser-driven proton of such high energies still remains to be demonstrated.

We have performed 2D large-scale PIC simulations with the code PICLS, to study the interaction of a high-intensity laser pulse with a cylinder and to see if the resulting expansion can be symmetric. In the experiments, the laser pulse interacts with a very localized region, but the resulting focusing is almost perfectly symmetrical.

The simulation box is 150 μm long and 150 μm wide.

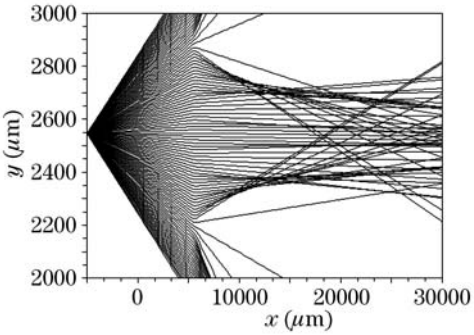

Fig. 2. Trajectories for 100 protons at 270 MeV entering the cylinder 22.9 ps before it is triggered. The cylinder is 6 mm long and the intensity of the laser pulse is 10^{20} W/cm^2. The pulse duration is 700 fs. The two axes are not scaled similarly for clarity.

The radius of the cylinder is 42 μm and its thickness is 6.4 μm. Plasma density is $10n_c$. The laser intensity is 3×10^{18} W/cm^2, and the pulse duration is 53 fs. The full width at half maximum (FWHM) of the laser pulse is 6 μm.

The simulated cylinder thickness is one fourth of the experimental cylinder thickness. Even with a smaller thickness, which is a source of dissymmetry, the expansion is remarkably symmetrical (Fig. 3), in agreement with experimental observations. The electrostatic field reaches 150 GV/m.

New experiments conducted at LULI using the same setup as the above for the secondary laser and the cylinder. Different cylinder parameters (radius and length) were used. The primary laser is used to produce a proton beam from a target with a grid attached close to its back surface to perform proton radiography of the fields inside the cylinder[11]. With this technique, images of the evolution of the field can be obtained with a picoseconds temporal resolution. Figure 4 shows an example of one of the images obtained. The field appears to be very symmetrical and the results are in very good agreement with the PIC simulation results with a laser interacting on a cylinder in a 2D geometry as explained above.

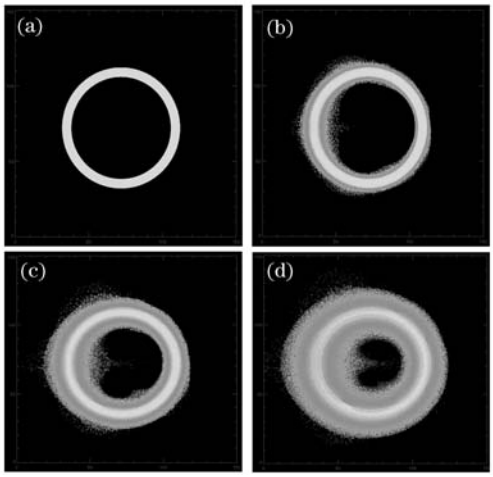

Fig. 3. Ion density for four different times during the expansion, (a) corresponds to the initial density, (b) corresponds to t = 12 ps after the beginning of the simulation, (c) corresponds to t = 24 ps after the beginning of the simulation, and (d) corresponds to t = 35 ps after the beginning of the simulation.

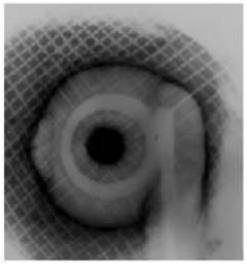

Fig. 4. RCF showing the angular distribution of 6-MeV protons that have transited through a cylinder (diameter 800 μm, length 470 μm) irradiated by a 3×10^{18}-W/cm^2, 320-fs laser pulse. These protons are accelerated by a 5×10^{19}-W/cm^2, 320-fs laser pulse.

The ultrafast laser-triggered micro-lens[7] provides tunable, simultaneous focusing and energy selection of MeV proton beams. We showed that this device could also focus very energetic proton beams (with a maximum proton energy higher than 200 MeV), if the parameters of the laser irradiating the cylinder are chosen carefully. 2D PIC simulations and new experiments were used to study the symmetry of the plasma expansion inside the laser-irradiated cylinder. The expansion is found to be symmetrical over very long time scales, in agreement with experimental observations.

We acknowledge fruitful discussions with L. Gremillet, T. Grismayer, S. Gordienko, and A. Pukhov. We thank the CEA/DAM for the simulations we performed on the CCRT computers. We acknowledge the expert support from the technical teams at LULI. This work has been supported by UNR Grant under DOE/NNSA Grant DE-FC52-01NV1405, EU-Grant No. HPRICT 1999-0052, Grant No. E1127 from Région Ile-de-France, and DFG TR18 and GK1203, and partly by the QUB-IRCEP scheme and DAAD. E. d'Humières's e-mail address is dhumieres@physics.unr.edu.

References

1. P. K. Patel, A. J. Mackinnon, M. H. Key, T. E. Cowan, M. E. Foord, M. Allen, D. F. Price, H. Ruhl, P. T. Springer, and R. Stephens, Phys. Rev. Lett. **91,** 125004 (2003).
2. R. Sonobe, S. Kawata, S. Miyazaki, M. Nakamura, and T. Kikuchi, Phys. Plasmas **12,** 073104 (2005).
3. R. A. Snavely, J. King, K. Akli, B. B. Zhang, R. Freeman, S. Hatchett, M. H. Key, A. MacKinnon, P. Patel, R. Town, S. Wilks, R. Stephens, R. Tsutsumi, Z. Chen, T. Yabuuchi, T. Kurahaski, T. Sato, K. Adumi, Y. Toyama, J. Zheng, R. Kodama, K. A. Tanaka, and T. Yamanaka, in *Proceeding of the IFSA 2003 Conference* (2003).
4. E. Fourkal, J. S. Li, M. Ding, T. Tajima, and C.-M. Ma, Med. Phys. **30,** 1660 (2003).
5. B. M. Hegelich, B. J. Albright, J. Cobble, K. Flippo, S. Letzring, M. Paffett, H. Ruhl, J. Schreiber, R. K. Schulze, and J. C. Fernandez, Nature **439,** 441 (2006).
6. H. Schwoerer, S. Pfotenhauer, O. Jäckel, K.-U. Amthor, B. Liesfeld, W. Ziegler, R. Sauerbrey, K. Ledingham, and T. Esirkepov, Nature **439,** 445 (2006).
7. T. Toncian, M. Borghesi, J. Fuchs, E. d'Humières, P. Antici, P. Audebert, E. Brambrink, C. A. Cecchetti, A. Pipahl, L. Romagnani, and O. Willi, Science **312,** 410 (2006).
8. L. Romagnani, J. Fuchs, M. Borghesi, P. Antici, P. Audebert, F. Ceccherini, T. Cowan, T. Grismayer, S. Kar, A. Macchi, P. Mora, G. Pretzler, A. Schiavi, T. Toncian, and O. Willi, Phys. Rev. Lett. **95,** 195001 (2005).
9. E. d'Humières, E. Lefebvre, and L. Gremillet, and V. Malka, Phys. Plasmas **12,** 062704 (2005).
10. E. Lefebvre, N. Cochet, S. Fritzler, V. Malka, M. M. Aléonard, J. F. Chemin, S. Darbon, L. Disdier, J. Faure, A. Fedotoff, O. Landoas, G. Malka, V. Méot, P. Morel, L. Rabec, M. Gloahec, A. Rouyer, C. Rubbelynck, V. Tikhonchuk, R. Wrobel, P. Audebert, and C. Rousseaux, Nucl. Fusion **43,** 629 (2003).
11. M. Borghesi, D. H. Campbell, A. Schiavi, M. G. Haines, O. Willi, A. J. MacKinnon, P. Patel, L. A. Gizzi, M. Galimberti, R. J. Clarke, F. Pegoraro, H. Ruhl, and S. Bulanov, Phys. Plasmas **9,** 2214 (2002).